Available online at www.sciencedirect.com

ScienceDirect

Procedia Engineering 213 (2018) 36–47

Procedia Engineering

www.elsevier.com/locate/procedia

7th International Conference on Fatigue Design, Fatigue Design 2017, 29-30 November 2017, Senlis, France

# Modeling and simulation of weld residual stresses and ultrasonic impact treatment of welded joints

Jing Zheng[a], Ayhan Ince[a,b*] and Lanqing Tang[a]

[a]*Purdue Polytechnic Institute, Purdue University, West Lafayette, IN 47906, USA*
[b]*Department of Mechanical, Industrial & Aerospace Engineering, Concordia University, Montreal, Quebec H3G 1M8, Canada*

**Abstract**

Most structures are fabricated using welded joints because of its low cost, structural strength and geometric flexibility. Welding is considered a highly complex metallurgical process that results in irregular geometries, material imperfections/flaws and tensile residual stresses. High tensile residual stresses and stress concentrations resulting from the weld process have a significant impact on fatigue life of structures, and thus a topic of great concern in product design. Ultrasonic impact treatment (UIT) is regarded as one of the most effective post welding treatment techniques to enhance the fatigue performance of welded structures. The UIT aims to introduce fatigue-beneficial compressive stresses by plastically deforming the weld toe and reduce stress concentrations by modifying local weld geometries. In this study, 3D modeling and simulation using finite element (FE) method has been performed to simulate welding process and numerical modeling of the UIT process to predict weld residual stress distribution of butt and T weld joints. The predicted numerical results under as-welded and UIT treatment conditions were compared to present weld residual stress improvements. Compared results shows that the UIT has potential applications on the fatigue design of welded structures, can lead to lighter structures and products, in which structures can be down-sized and optimized to reduce weights.


Peer-review under responsibility of the scientific committee of the 7th International Conference on Fatigue Design.

*Keywords:* Ultrasonic impact treatment (UIT), finite element modeling (FEM), weld residual stress, weld process

## 1. Introduction

Welding technology has been widely applied in the fields of automobile, aviation, nuclear, vessel manufacturing and other industrial sectors due to its low cost, geometrical flexibility and desirable mechanical properties [1]. On the other hand, welding comes with the expense of some detrimental effects on welded structures such as micro-cracks/flaws, high stress concentration and tensile residual stresses. Hence, from the point view of fatigue design, welded areas are deemed as weak structural joints where cracks and tensile residual stresses are easily to be found [2]. Over the past several decades, numerous post-weld treatment techniques, including grinding, TIG dressing, hammer peening and shot peening, have been developed to address this vexing issue and improve fatigue

1877-7058 
Peer-review under responsibility of the scientific committee of the 7th International Conference on Fatigue Design.
10.1016/j.proeng.2018.02.005

performance of weld joints, [3]. These treatments are generally classified into two different categories: geometry improvement and residual stress modification techniques. Geometry improvement techniques such as TIG dressing and grinding focus on eliminating flaws and reducing stress concentration of welded components. While residual stress modification techniques like hammer peening and shot peening lay emphasis on introducing beneficial compressive residual stresses and improving residual stress distributions of welded joints[4].

Ultrasonic impact treatment (UIT) is a recently developed treatment technique by Statnikov et al. in former Soviet Union [5]. This technique has become increasingly popular for several reasons such as reducing manpower requirements, eliminating the weld induced distortions. The UIT uses needles or hammer-like rods to impact the welding surface/toe at a high ultrasonic frequency of 18000-27000 Hz. The UIT, not only reduces the local stress concentration by modifying the weld toe geometry but also introduces compressive residual stresses by eliminating tensile residual stresses [6].

In recent years, numerous studies have been carried out to investigate the effect of the UIT on the weld residual stresses and fatigue performance of weld joints [7-10]. Numerical models have been developed to predict the residual stress distribution and fatigue performance of UIT-treated weld joints [9, 11]. Meanwhile, experimental studies of the UIT have been also conducted [7-8, 10]. Various measurement techniques such as X-ray diffraction and neutron diffraction were used to obtain experimental data for the validation of simulated residual stresses. In most of the cases, it has been found that the UIT introduces compressive residual stresses along varying depths and improves fatigue performances of weld joints in various extent. Turski et al. [7] found that the UIT produced compressive residual stress fields of about 2mm in depth for 304 stainless steel. Liu et al. [8] measured residual stresses of UIT-treated high strength steel weld joints. The results indicated that the UIT had the same effect on both longitudinal and transverse stresses and introduced a compressive residual stress layer up to 4mm in depth. Foehrenbach et al. [9] developed a computationally efficient approach to predict residual stresses induced by the UIT process using a commercial finite element software package. It was found that compressive residual stresses up to a base material yield strength occurred after the UIT treatment. Dekhtyar et al. [10] studied the effect of the UIT on fatigue behavior of Ti–6Al–4V specimens. Based on experimental data, it can be revealed that the UIT introduced compressive stresses of -570MPa, achieving two thirds of yield limit of the material. Fatigue strength of as-welded joints were increased by 60% at $10^7$ cycles and fatigue life was extended $10^2$ times at stress amplitude of 300 MPa.

To assess fatigue life improvement by the UIT treatment, it is necessary to accurately estimate residual stress distribution through finite element analysis (FEA). Recent numerical studies emphasized on the influence of mesh type, material properties, boundary conditions, pin tool size, modeling strategy and material hardening rules on computed numerical results [9, 11-12]. It was well know that the isotropic hardening model is valid for monotonic loading [9]. However, due to the Bauschinger effect, isotropic hardening model is not suitable for cyclic loadings experienced under of the UIT process [13]. On the other hand, linear kinematic hardening model could be applied to describe material behavior under cyclic loading conditions, but it could provide reasonable results for small strains loading conditions [14]. Therefore, the combined isotorpic-kinematic hardening model, or Chaboche model was resulted from the UIT simulation [15-16]. In addition, in the modeling of the UIT process, regardless the complex components and ultrasonic transducer of the UIT device, the pin impact can be simplified as the movement of the impact pin tool given proper controlling parameters. These parameters consist of impact velocity, the contact force and the pin displacement. Hence, modeling strategies of the UIT can be classified into three categories: velocity-controlled simulation (VCS), force-controlled-simulation (FCS) and displacement-controlled-simulation (DCS) [17-19]. In the VCS strategy, the velocity of the impact pin can be obtained through the approximated motion using a sinusoidal harmonic function, where the first derivative represents the velocity [17]. The FCS strategy defines the pin impact with a given load force while the DCS utilizes the permanent indentation obtained by the UIT to define the displacement of the pin [18-19].

This paper focuses on effects of the UIT on residual stresses of 304L weld joints. FE analysis was carried out to simulate residual stress distributions of as-welded and the UIT treated joints.

## 2. Finite element numerical modeling

### *2.1. Finite element modeling of welding process*

Finite element (FE) simulations of the butt and T weld joints were performed using ABAQUS software package to predict the residual stresses induced by welding process. As shown in Fig.1, due to the overall symmetry, only one-half of the weld joints was modeled for both butt and T weld joints. The eight-node Hex element C3D8T was employed to model welding geometry and refined meshes were created in the vicinity of the weld region to obtain more accurate results. The minimum element size was selected as 1 mm × 1 mm × 1 mm in the weld zone. The total number of nodes is 251585 for butt joint and 240692 for T-joint. Specific paths in various directions were chosen to analyze the residual stress distributions of weld joints in Fig. 2. Boundary surfaces were exposed to both radiation and convection condition, with emissivity of 0.85 and filming coefficient of 10w/ (m2℃). Mechanical boundary conditions were applied on the FE model, seen in Fig. 2. In the butt joint, path H-G was constrained in Z-direction, path I-H and G-J were restricted in Y-direction, and nodes on the symmetry plane were constrained in X-direction. Similarly, in T-joint, path F-G was constrained in Z-direction, path G-H and F-I was constrained in Y-direction, and nodes on the symmetry plane were restricted in X-direction. In this paper, material properties of heat affected zone (HAZ), the weld metal and the base metal were assumed the same. Temperature-dependent material properties were obtained from the previous research works [20], as shown in Fig.3.The double ellipsoidal heat source model was applied for welding simulation [21], which was expressed as a heat flux function.

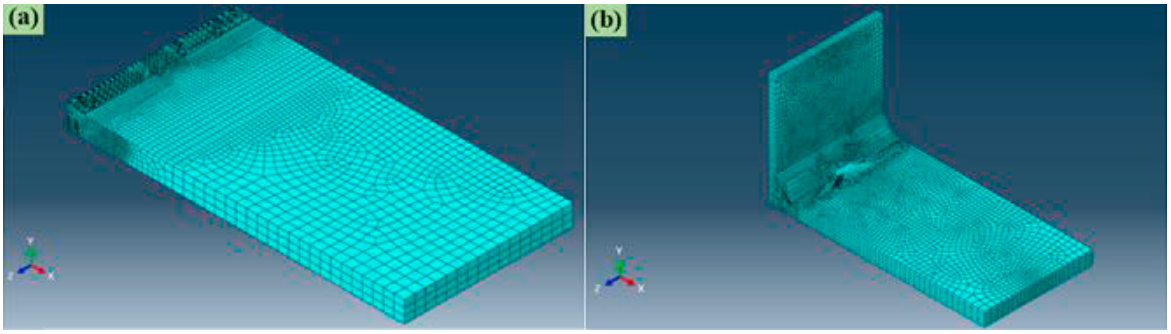


Fig. 1 3-D finite element model: (a) butt joint, (b) T-joint.

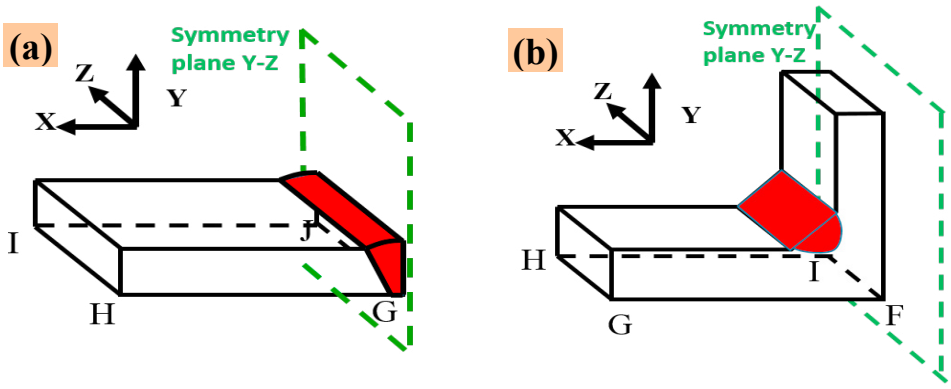


Fig. 2 3-D finite element model: (a) butt joint, (b) T-joint.

### 2.2. Finite element modeling of ultrasonic impact treatment

A fully dynamic numerical model using ABAQUS code was performed to simulate the UIT process. The UIT simulation was performed by importing predicted welding residual stresses as the initiate initial state. An Impact zone with dense meshes were created in the middle of welding zone, where peak tensile residual stress usually occurred, as shown in Fig.3. The minimum element size in the impact zone was selected as 0.1mm ×0.1mm × 0.5mm. The combined isotropic kinematic material plasticity model was utilized for the UIT simulation. The corresponding material parameters of the plasticity model were obtained from existing data [14] shown in Table 1.

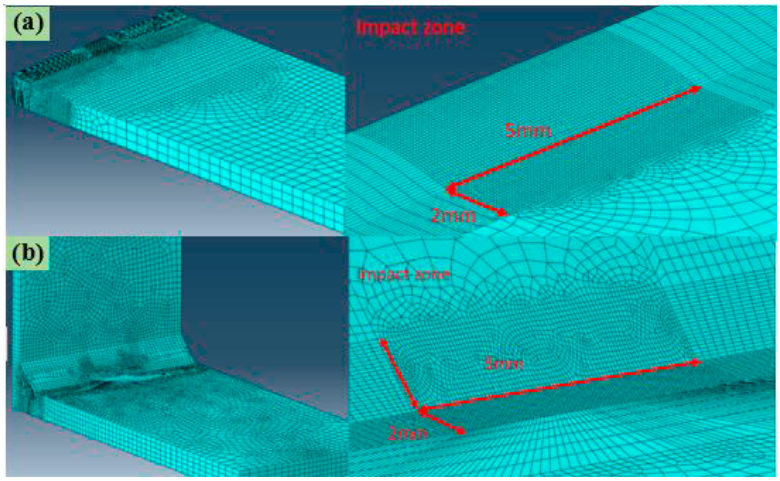


Fig.3 Impact zone of UIT simulation: (a) butt joint, (b) T-joint

Table 1 Calibrated Chaboche model parameters for 304L (Le Pécheur et. Al, 2012)

| E(GPa) | υ | $\sigma_{ys}$(MPa) | $C_1$ (MPa) | $\gamma_1(s^{-1})$ | $C_2$ (MPa) | $\gamma_2(s^{-1})$ |
|---|---|---|---|---|---|---|
| 194 | 0.3 | 250 | 20.0 | 10.0 | 12613 | 0.015 |

The displacement-controlled simulation (DCS) strategy was adopted to control the movement of the pin impact. As depicted in Fig.4, the permanent indentation, the diameter of pin head ,the angle of pin for butt joint and T-joint were set to 0.1mm, 3mm, 75° and 67.5°, respectively. The pin model was defined as a rigid body. The pin tool was set to move along the welding direction and impact on the surface of the weld joint at intervals of 0.3 mm, which was chosen to realistically represent the actual UIT process, as seen in Fig.4.

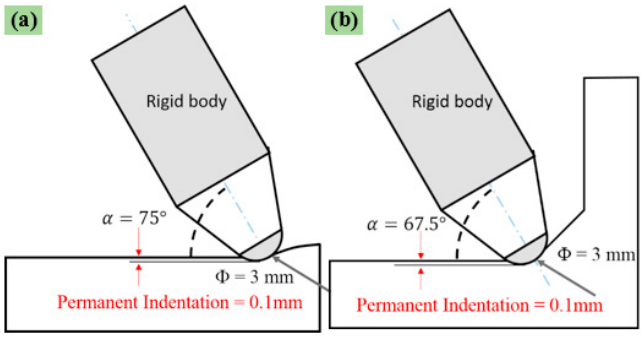


Fig. 4 Pin tool position and indentation: (a) butt joint, (b) T-joint

## 3. Results and Discussions

As for weld residual stress predictions for the weld and UIT processes, A-B, A-C and A-D paths in Figs 5-10 were chosen to analyze residual stress distributions of welding butt and T joints. Figure 2 demonstrates residual stress directions of both weld joints. Three definite words “longitudinal”, “transverse” and “through-thickness” were introduced to describe residual stresses in three-dimensional space. The transverse residual stress,$\sigma_{xx}$, indicated residual stress in direction perpendicular to the weld line. The longitudinal stress,$\sigma_{zz}$, depicted stress in direction parallel to the weld line and through-thickness stress, $\sigma_{yy}$, demonstrated stress in the depth direction.

### *3.1. Residual stress predictions in weld butt-joint*

The predicted residual stresses obtained from the numerical model were compared with experimental data [22] to verify predicted results of butt weld joint. Figures 5 -6 demonstrate predicted and measured residual stress distributions in the butt weld joint along paths of the A-B and A-C , respectively. The red markers shown in Fig. 5-6 indicate the experimental residual stress data measured by the XRD method [22]. As shown in Fig. 5, the distributions and magnitude of experimental residual stress were approximately consistent with the predicted results in the A-B path. Generally, both peak transverse residual stress and longitudinal residual stress appeared in the vicinity of weld zone. The stress components, $\sigma_{xx}$ and $\sigma_{zz}$ decreased with the increasing distance from the point A and levelled out to zero.

On the other hand, Fig. 6 shows that the simulated residual stresses shared the same trend with the experimental one along the A-C path. However, there were some differences in residual stresses obtained from the experiment [22] and those predicted by the FEA. Those differences were attributed to erroneous measurements of the XRD method, which was sensitive to the microstructure evolution of welding zone [6]. At each end of the A-C path, experimental transverse residual stresses were relatively smaller than the simulated results. However, the experimental transverse residual stress (275 MPa) were significantly higher than the simulated ones (172 MPa) at the middle of the A-C path..

Based on presented results, the predicted results by the FE analysis were in good agreement with the experimental data. That is to say, the FE model can predict the residual stress distributions of welded joints with reasonable accuracy.

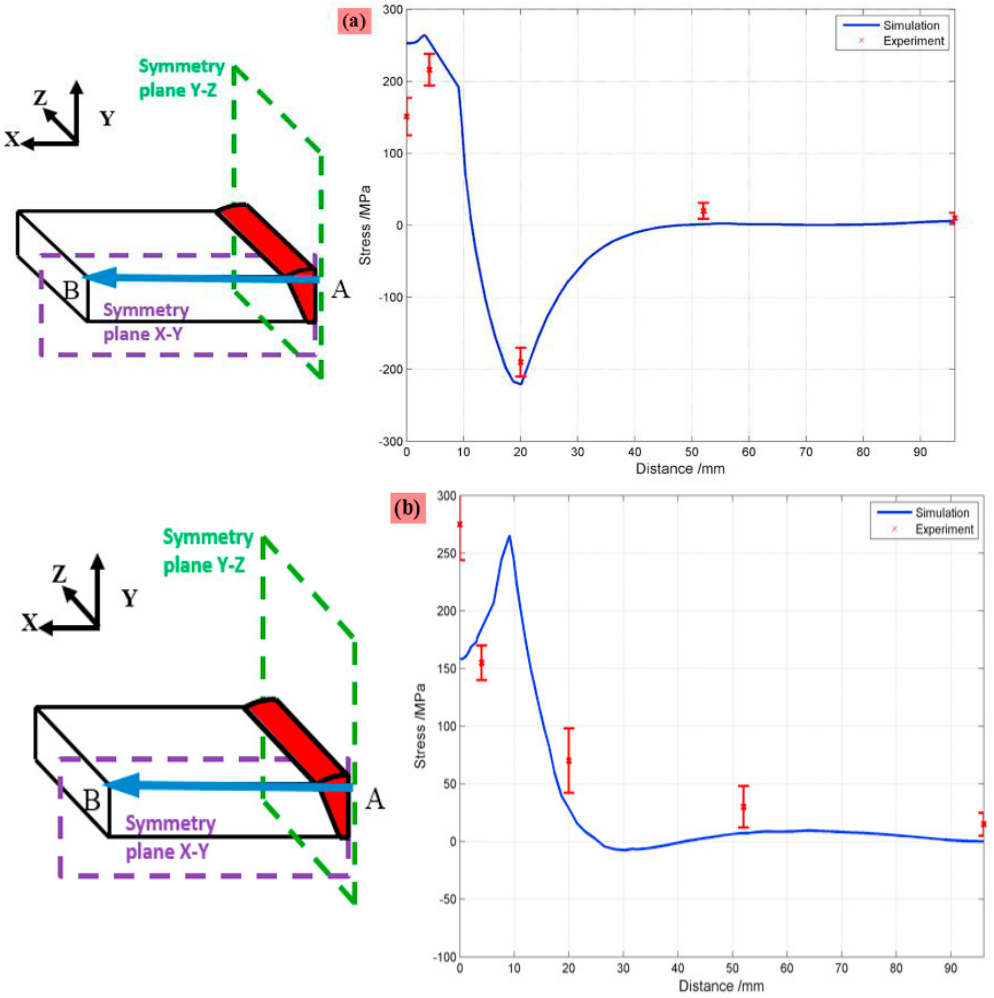


Fig. 5 Transverse (a) and longitudinal (b) residual stress distributions along A-B path in butt welded joints

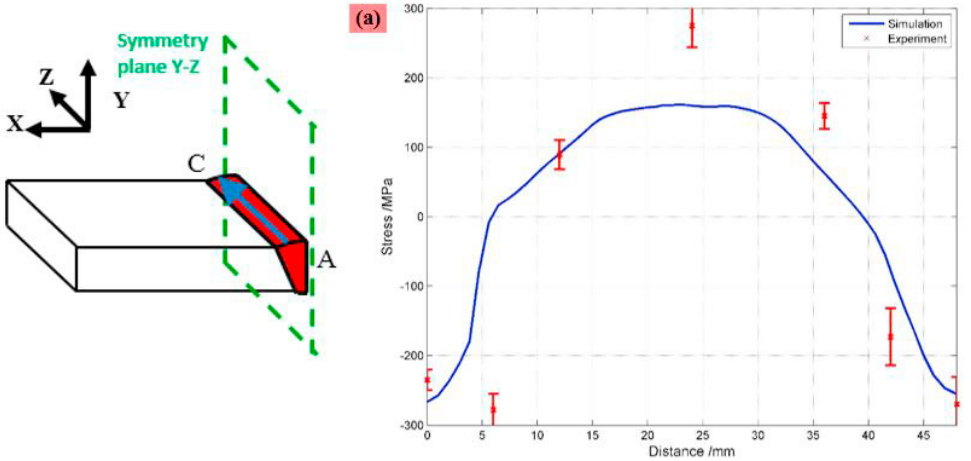


Fig. 6 Transverse residual stress distributions along A-C path in butt welded joints

### *3.2. Residual stress predictions in weld T-joint*

In welding simulation, A-B and A-C paths were chosen to analyze residual stress distributions of welding T-joint. Figures 7-8 demonstrate residual stress distributions of butt and T joints along paths of the A-B and A-C. Longitudinal and transverse residual stresses of T-joint along the A-B path are plotted in Fig.7. It can be observed that both the transverse residual stress $\sigma_{xx}$ and the longitudinal residual stress $\sigma_{zz}$ reached peak values near the weld region where the highest resistance occurred during the welding process. However, after reaching the maximum values, $\sigma_{xx}$ and $\sigma_{zz}$ reflected a different trend in the A-B path. As shown in Fig. 7(a), $\sigma_{xx}$ monotonically decreased with the distance from the point A. whereas, with the increasing distance from point A, $\sigma_{zz}$ decreased from tensile stresses into compressive ones and then increased to zero value, as seen in Fig. 7(b). In the region far from the welding zone, both transverse and longitudinal residual stresses decreased to negligible values with the increase of distance from the welding zone, which were similar to results of previous studies [30-31].

Figure 8 presents transverse and longitudinal residual stress distributions of T-joints along the A-C path. Apparently, both transverse residual stresses $\sigma_{xx}$ and longitudinal residual stresses $\sigma_{zz}$ showed a similar trend along the A-C path. In the middle of the weld line (point A), $\sigma_{xx}$ and $\sigma_{zz}$ reached peak tensile stress values. The peak values of $\sigma_{xx}$ and $\sigma_{zz}$ were 350MPa and 200MPa, respectively. As the distance from point A increased, $\sigma_{xx}$ and $\sigma_{zz}$ decreased gradually, changing from tensile stresses into compressive stresses.

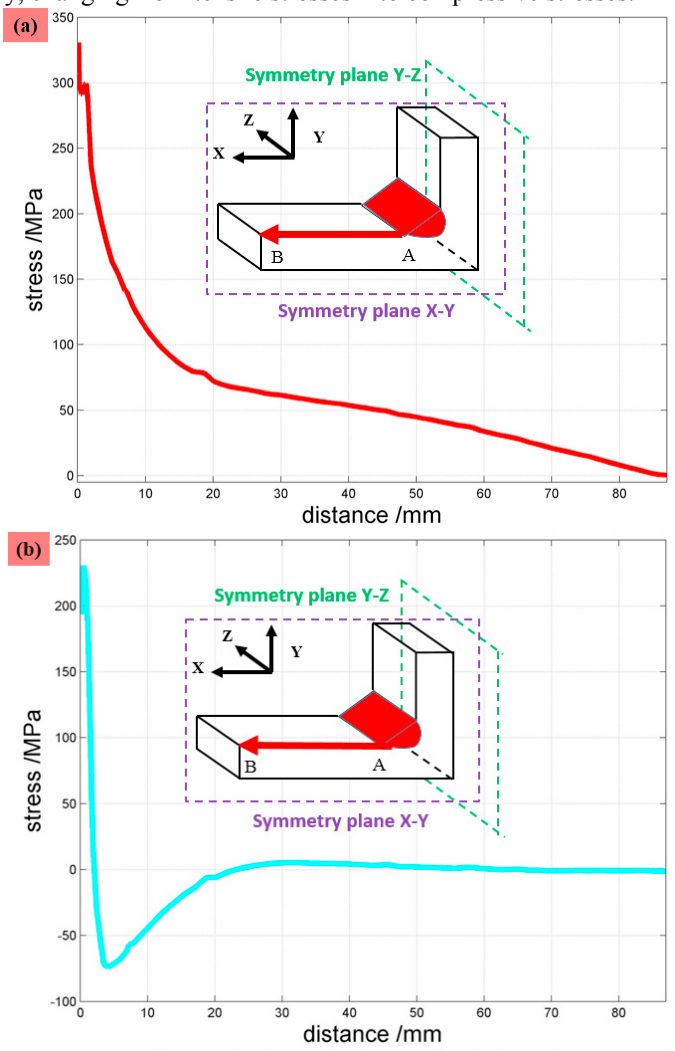


Fig. 7 Transverse (a) and longitudinal (b) residual stress distributions along A-B path in T-joints

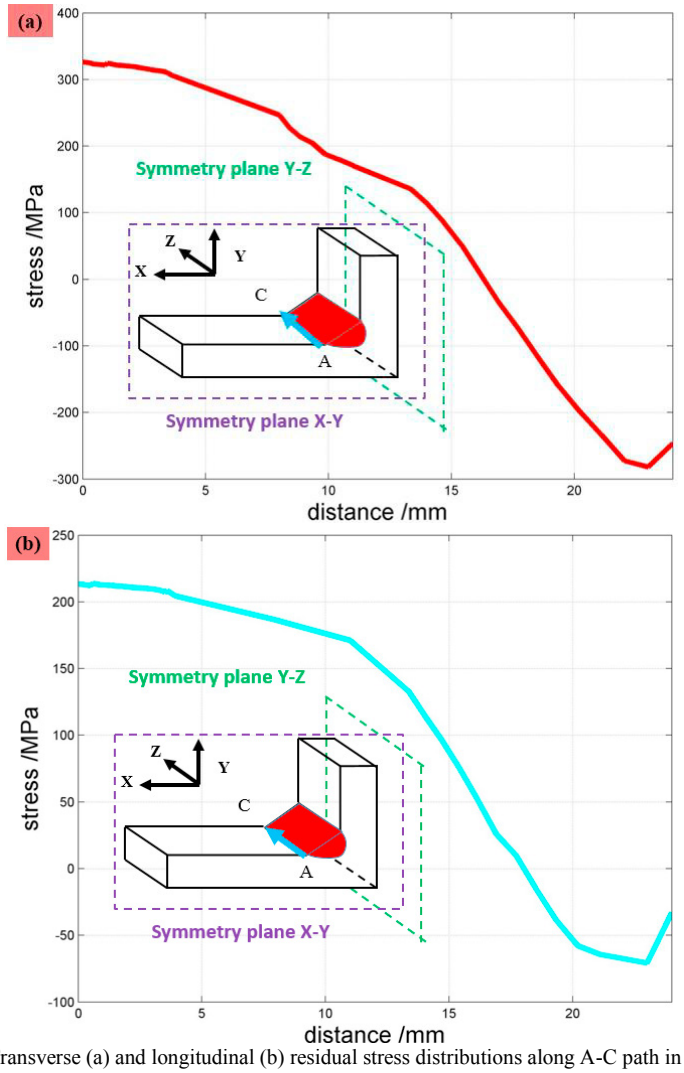


Fig. 8 Transverse (a) and longitudinal (b) residual stress distributions along A-C path in T-joints

### *3.3. Effects of UIT on weld residual stresses*

To study effect of the UIT on residual stress distribution in the depth direction (A-D path), the simulated results of residual stresses for as-welded model were compared with those for the UIT treated model. Fig. 9 and Fig. 10 demonstrate residual stress distribution in A-D path of T-joint and butt joint, respectively. As for butt joint, the stress components, $\sigma_{xx}$, $\sigma_{yy}$ and $\sigma_{zz}$ changed smoothly as the depth increased, with average stresses of 189 MPa, 9MPa and 267MPa, respectively in Fig. 9. In case of the T-joint, before the UIT, high tensile residual stresses up to the yield strength appeared on the upper surface of as-welded joint, shown Fig. 10. The residual stresses reached their maximum tensile levels near the upper surface and then decreased with the increasing depth. The peak values of $\sigma_{xx}$, $\sigma_{zz}$ and $\sigma_{yy}$ appeared near the upper surface were 372 MPa, 364 MPa and 151 MPa, separately. Owing to small constrain in in Y-direction, $\sigma_{yy}$ tended to show a lower value than $\sigma_{xx}$ and $\sigma_{zz}$. After the UIT,$\sigma_{xx}$, $\sigma_{yy}$ and $\sigma_{zz}$ changed into compressive stresses near the upper surface of weld joint. Compared to $\sigma_{xx}$and $\sigma_{yy}$, $\sigma_{zz}$ had higher compressive values due to the overlapping of the UIT in longitudinal direction. The maximum compressive stresses in the longitudinal direction ($\sigma_{zz}$) of butt and T joints were -375MPa and -312MPa and, respectively, which were higher than the compressive yield limit of 304L steel, seen in Fig. 9(b) and 10(b). This implied cold working by the

UIT induced plastic deformation of the weld joint. The same level of residual stress exceeding the yield stress of material was also measured by previous researchers [7, 28].

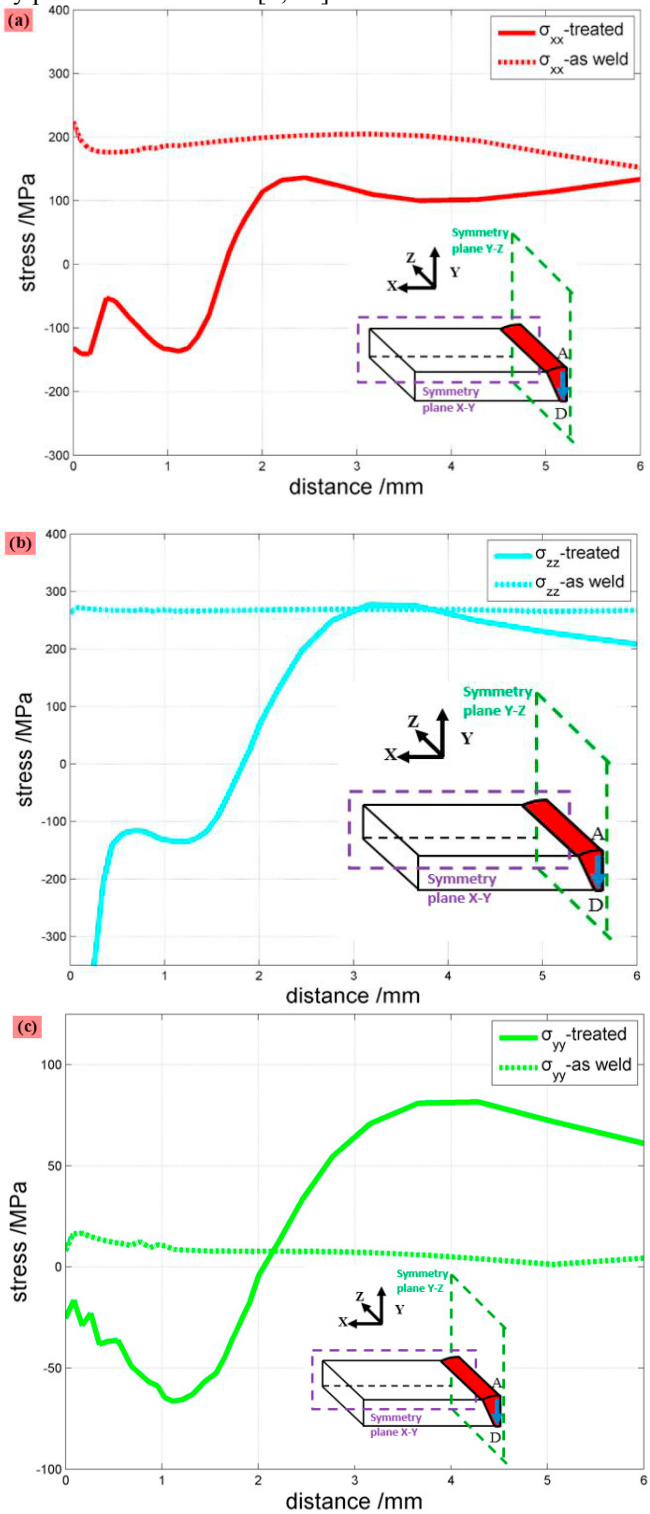


Fig. 9 Transverse (a), longitudinal (b) and through-thickness(c) residual stress distributions along A-D path in as-welded and UIT-treated butt joints

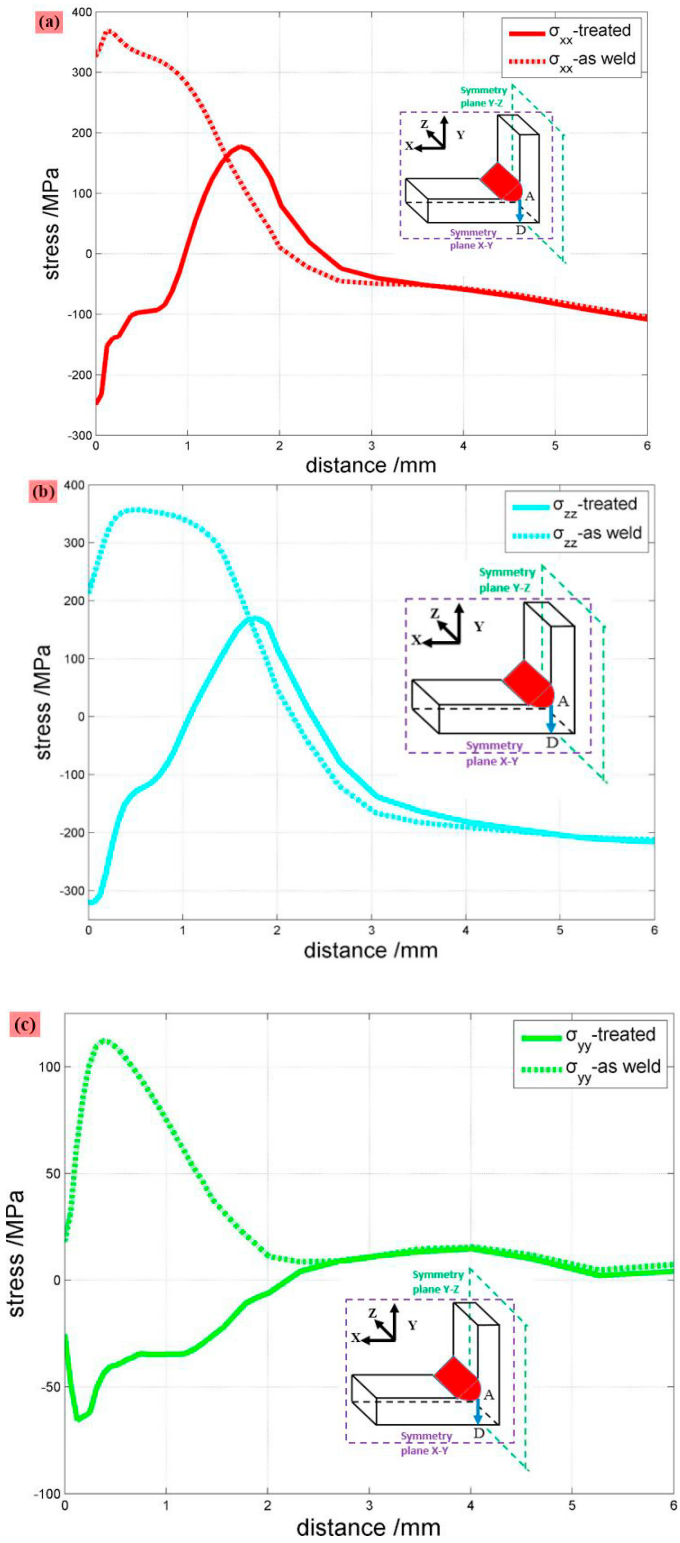


Fig. 10 Transverse (a), longitudinal (b) and through-thickness(c) residual stress distributions along A-D path in as-welded and UIT-treated T-

Additionally, the effect of the UIT faded with the increasing depth. For T-joint, the depths of the UIT treated compression layer of $\sigma_{xx}$, $\sigma_{zz}$ and $\sigma_{yy}$ were 2.3 mm, 2.5mm and 3.1mm, respectively. In terms of butt joint, compressive stresses of three directions were introduced to up to 2mm in the depth. Similar results were also reported, in which compressive residual stress layer of 2-3mm depth were generated by the UIT [29]. The results above demonstrated that the UIT introduced compressive stresses in the upper surface of weld joints, which had a beneficial effect on fatigue strength of material [3, 29-31].

The local stresses and strains including weld residual stresses have defense and aerospace applications have particularly importance to assess fatigue performance of critical welded components/structures in defense, automotive and aerospace applications [32-33]. Omission of weld residual stresses may cause irreversible catastrophic failures once one of those components fail.

## Conclusions

The current study investigated effects of the UIT on residual stresses of 304L stainless steel weld joints. Both welding and UIT processes for butt and T joints were simulated using the FEA. Experimental data was used to validate the predicted residual stress field of the butt joint. Based on the predicted numerical and experimental results presented, conclusions can be drawn as follows.

- The results of residual stresses indicated that both the transverse and longitudinal residual stresses reached peak tensile values near the weld toe region. Away far from the welding zone, residual stresses decreased to negligible values.
- Experimental the residual stresses for butt joints were in good agreement with the predicted FE results. It was found that the FE model could predict the residual stress distributions of weld joints with reasonable accuracy.
- The UIT introduced beneficial compressive residual stresses at weld joints and the maximum compressive stresses exceeded the compressive yield limit of 304L stainless steel. In addition, the effect of the UIT faded with the increasing depth at the weld toe. The depths of the UIT treated compression layer of T-joint and butt joint were up to 3mm and 2mm, respectively.
- Residual stress results demonstrated that the UIT could remarkably extend fatigue lives of weld joints.

## References

[1] T. L. Teng, C. P. Fung, P. H. Chang, W. C. Yang, Analysis of residual stresses and distortions in T-joint fillet welds, International Journal of Pressure Vessels and Piping, 2001(78) 523-538.
[2] I. Weich, U. Thomas, N. Thomas, K. Dilger, H. E. Chalandar, Fatigue behavior of welded high-strength steels after high frequency mechanical post-weld treatments, Weld World, 53(2009) R322-R332.
[3] R. Rakesh, K. Ghahremani, S. Walbridge, A. Ince, Testing and fracture mechanics analysis of strength effects on the fatigue behavior of HFMI-treated welds, Weld World, 60(2016) 987-999, DOI: 10.1007/s40194-016-0354-4.
[4] G.B. Marquis, E. Mikkola, H.C. Yildirim, Z. Barsoum, Fatigue strength improvement of steel structures by high-frequency mechanical impact: proposed fatigue assessment guidelines, 57(2013) 803-822.
[5] E.S. Statnikov, Applications of operational ultrasonic impact treatment (UIT) technologies in production of welded joints, Welding in the World, 44(2000) 11-21.
[6] D. Deng, H. Murakawa, Numerical simulation of temperature field and residual stress in multi-pass welds in stainless steel pipe and comparison with experimental measurements, Computational Materials Science, 37 (2006) 269-277.
[7] M. Turski, S. Clitheroe, A.D. Evans, C. Rodopoulos, D.J. Hughes, P.J. Withers, Engineering the residual stress state and microstructure of stainless steel with mechanical surface treatments, Applied physics a-materials science & processing, 99(2010) 549-556.
[8] Liu, Q. Ge, D.J. Chen, F. G, J.S. Zou, Residual stress variation in a thick welded joint after ultrasonic impact treatment, Science and Technology of Welding and Joining,21(2016) 634-631.
[9] J. Foehrenbach, V. Hardenecke, M. Farajian, High frequency mechanical impact treatment (HFMI) for the fatigue improvement: numerical and experimental investigations to describe the condition in the surface layer, Welding in the World. 60(2016) 749-755.
[10] A.I. Dekhtyar, B.N. Mordyuk, D.G. Savvakin, V.I. Bondarchuk, I.V. Moiseeva, N.I. Khripta, Enhanced fatigue behavior of powder metallurgy Ti–6Al–4V alloy by applying ultrasonic impact treatment, Materials Science and Engineering: A, 641(2015) 348-359.
[11] C.B. Guo, Z.J. Wang, D.P. Wang, Numerical analysis of the residual stress in ultrasonic impact treatment process with single-impact and two-impact models, Applied Surface Science, 347(2015) 596-601.
[12] B.N. Mordyuka, M.O. Iefimovb, G.I. Prokopenkoa, T.V. Goluba, M.I. Danylenkob, Structure, microhardness and damping characteristics of Al matrix composite reinforced with AlCuFe or Ti using ultrasonic impact peening, Surface and Coatings Technology, 204(2010) 1590-1598.
[13] O. Muránskya, C.J. Hamelina, M.C. Smithb, P.J. Bendeicha, L. Edwardsa, The effect of plasticity theory on predicted residual stress fields in numerical weld analyses, Computational Materials Science, 54(2012) 125-134.
[14] A. Le Pécheura, F. Curtitb, M. Clavela, J.M. Stephanb, C. Reya, Ph. Bomparda, Thermo-mechanical FE model with memory effect for 304L austenitic stainless steel presenting microstructure gradient, International Journal of Fatigue, 45(2012) 106-115.
[15] A.H. Mahmoudi, S.M. Pezeshki-Najafabadi, H. Badnava, Parameter determination of Chaboche kinematic hardening model using a multi objective Genetic Algorithm, Computational Materials Science, 50(2011) 1114-1122.
[16] J.L. Chaboche, A review of some plasticity and viscoplasticity constitutive theories, International Journal of Plasticity, 24(2008) 1642-1693.
[17]X.J. Yang, J.X. Zhou, X. Ling, Study on plastic damage of AISI 304 stainless steel induced by ultrasonic impact treatment, Material & Design, 36(2012) 477-481.
[18] K.L. Yuan, Modelling of ultrasonic impact treatment (UIT) of welded joints and its effect on fatigue strength, Frattura ed Integrità Strutturale,34(2015) 476-486.
[19] H. Zheng, D. F. Liu, C. F. Lee, L.G. Tham, Displacement-controlled method and its applications to material non-linearity, International Journal for Numerical and Analytical Methods in Geomechanics, 29(2005) 209-226.
[20] L.Q. Tang, H.F. Li, X.X. Wang, C.F. Qian, Numerical simulation and experimental investigation of residual stress in 06cr19ni10 austenitic stainless steel weld joint with effects of strain-strengthening. Applied Mechanics and Materials, 853(2017) 204-208.
[21] J. Goldak, A. Chakravarti, M. Bibby, A new finite element model for welding heat sources, Metallurgical Transactions B, 15(1984) 299-305.
[22] J. Zheng, A. Ince, Numerical modeling and simulation of welding residual stresses using finite element method, 8th International Conference on Physical and Numerical Simulation of Materials Processing (ICPNS), Seattle, Washington (2016).
[23] W. Liang, H. Murakawa, D. Deng, Investigation of welding residual stress distribution in a thick-plate joint with an emphasis on the features near weld end-start, Materials & Design, 67(2015) 303-312.
[24] D.J. Smith, S.J. Garwood, Influence of postweld heat treatment on the variation of residual stresses in 50 mm thick welded ferritic steel plates, International Journal of Pressure Vessels and Piping, 51(1992) 241-256.
[25] A. Mitra, N. S. Prasad, G.D. J. Ram, Estimation of residual stresses in an 800 mm thick steel submerged arc weldment, Journal of Materials Processing Technology, 229(2016) 181-190.
[26] J.J. Xu, Z.Q. Zhu, L.G. Chen, C. Z. Ni, Temperature distribution and residual stresses during multipass narrow gap welding of thick plates, Materials Science and Technology, 22(2006) 232-237.
[27] S.D. Ji, H.Y. Fang, X.S Liu, Q.G. Meng, Influence of a welding sequence on the welding residual stress of a thick plate, Modelling & Simulation in Materials Science & Engineering, 13(2005) 553-566.
[28]S. Roy, J.W. Fisher, B.T. Yen, Fatigue resistance of welded details enhanced by ultrasonic impact treatment (UIT), International Journal of Fatigue, 25(2003) 1239-1247.
[29]K. Yuan, Y. Sumi, Simulation of residual stress and fatigue strength of welded joints under the effects of ultrasonic impact treatment (UIT), International Journal of Fatigue, 92(2016) 321-332.
[30]Y. Liu, D.P. Wang, C.Y. Deng, L.Q. Xia, L.H. Huo, L.J. Wang, B.M. Gong, Influence of re-ultrasonic impact treatment on fatigue behaviors of S690QL welded joints, International Journal of Fatigue, 66(2014) 155-160.
[31] K. Ghahremani, R. Ranjan, S. Walbridge, A. Ince, Fatigue strength improvement of aluminum and high strength steel welded structures using high frequency mechanical impact treatment, Procedia Engineering, 113(2015) 465-476, DOI: 10.1016/j.proeng.2015.12.616.
[32] A. Ince, A novel technique for multiaxial fatigue modelling of ground vehicle notched components, International Journal of Vehicle Design, 67(2015) 294–313, DOI: 10.1504/IJVD.2015.069486.
[33] A. Ince, A Computational Multiaxial Model for Stress-Strain Analysis of Ground Vehicle Notched Components. SAE International Journal of Engines, 10(2017) 316-322, DOI: 10.4271/2017-01-0329.